Journal Name

COMMUNICATION

Evidence for Diffusing Atomic Oxygen Uncovered by Separating Reactants with a Semi-Permeable Nanocapsule Barrier

Received 00th January 20xx,
Accepted 00th January 20xx

DOI: 10.1039/x0xx00000x

www.rsc.org/

Sara M. Omlid,[a] Sergey A. Dergunov,[b] Kathryn L. Sulkowski,[a] Ankita Isor,[a] John T. Petroff II,[a] Eugene Pinkhassik,[b] Ryan D. McCulla*[a]

Ground-state atomic oxygen [O(^{3}P)] is an oxidant whose formation in solution was proposed but never proven. Polymer nanocapsules were used to physical separate dibenzothiophene *S*-oxide (DBTO), a source of O(^{3}P), from an O(^{3}P)-accepting molecule. Irradiation of polymer nanocapsules loaded with DBTO resulted in oxidation of the O(^{3}P)-acceptor placed outside nanocapsules. The results rule out a direct oxygen atom transfer mechanism, effectively identifying the freely diffusing oxidant as O(^{3}P).

Ground state atomic oxygen, O(^{3}P), is a reactive oxygen species and the smallest diradical known. The UV irradiation of dibenzothiophene *S*-oxide (DBTO) results in unimolecular S—O bond cleavage to form dibenzothiophene (DBT) and an oxidant whose reactivity resembles that of O(^{3}P). A bimolecular mechanism of deoxygenation, generating other reactive oxygen species such as $^1O_2$, was inconsistent with the experimental findings.[1,2] However, to date it has not been possible to rule out a viable "oxenoid" alternative involving oxygen atom transfer directly from DBTO.[1,2] In the absence of steric burdens within the molecule to be oxidized, the reactivities of the conceivable oxidants are expected to be indistinguishable. Thus, a key mechanistic question is whether the observed oxidations are the result of a freely diffusing oxidant, namely O(^{3}P), or oxygen atom transfer directly from DBTO.

The absence of spectroscopic techniques for condensed-phase detection is an obstacle in studying very small and relatively short-lived intermediates such as O(^{3}P). Kautsky and de Brujin faced the same problem in their efforts to uncover singlet oxygen.[3,4] Their solution was a "three-phase test" involving the photosensitizer dye, trypaflavine, and an oxygen acceptor dissolved separately on SiO_2 gel beads, which allowed for a millimeter of air separating the two molecules. By physically separating the site of oxidant generation from the site of oxidation, the experiment elegantly demonstrated that the oxidant produced upon irradiation was capable of diffusing through air.

A challenge for highly reactive oxidants like O(^{3}P) is the need for very short distances between reactants, which cannot be achieved with Kautsky's three-phase test. Porous shells of polymer nanocapsules offer a barrier in solution, capable of physically separating relatively large molecules while allowing for the diffusion of small molecules through very small pores (diameter, <1 nm) in the nanocapsule shell.[5] Small-angle neutron scattering revealed that the thickness of the shells in these vesicle-templated capsules is 1.0 ± 0.1 nm.[6] Long-term stability studies of nanocapsules showed no measurable efflux of molecules larger than the pore size over five years.[7,8] For example, nanocapsules loaded with pH–sensitive indicator dyes showed unhindered transport of protons while being impermeable to molecules larger than the pore size.[9,10]

We designed an experiment involving the irradiation of DBTO-loaded nanocapsules in the presence of an O(^{3}P) acceptor molecule, referred to as an O(^{3}P)-trap, the nanocapsules act as a barrier that only allows passage of the putative O(^{3}P), or other freely diffusing small oxidant, through the small holes (or pores) of the nanocapsule shell. Therefore, if the oxidation mechanism involved only oxygen atom transfer from DBTO, the barrier would prevent oxidation of the O(^{3}P)-trap. Following photolysis, the formation of oxidized O(^{3}P)-trap would confirm a freely diffusing oxidant.

The most efficient method of encapsulating molecules within nanocapsules was to use water-soluble molecules.[11,12] Therefore, we prepared a water-soluble DBTO derivative (**1a**).[13] The functionalization was shown to have no significant ameliorating effect on photodeoxygenation properties (Table S1). The optimal O(^{3}P)-trap, **2a**, was synthesized using a known procedure.[14] **2a** offered three sulfides, which are known to have high reaction rate constants with O(^{3}P);[15-17] symmetry, which allowed for a single oxidation product; and aromatic groups, which allowed for UV detection. An authentic sample of the anticipated O(^{3}P) oxidation product, **2b**, was synthesized

---

[a] *Department of Chemistry, Saint Louis University, 3501 Laclede Ave. St. Louis, MO 63103 USA.*

[b] *Department of Chemistry, University of Connecticut, 55 North Eagleville Road, Storrs, CT 06269 USA.*

Electronic Supplementary Information (ESI) available: [details of any supplementary information available should be included here]. See DOI: 10.1039/x0xx00000x through the oxidation of **2a** by traditional means (i.e. using mCPBA). As shown in Figure 1, irradiation of **1a**-loaded nanocapsules would only be expected to yield **2b** if a freely diffusing oxidant was generated.

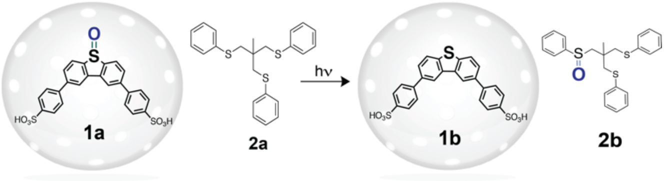

Figure 1. Experimental design: using the photolysis of **1a**-loaded nanocapsules in the presence of **2a** to provide evidence for a freely diffusing oxidant.

The synthesis of polymer nanocapsules was accomplished using an aqueous suspension of self-assembled vesicles as templates with bilayers loaded with hydrophobic monomers and cross-linkers as scaffolds. Nanocapsules were constructed from vesicle templates which formed spontaneously in water with appropriate concentrations of surfactants,[12,18] which were 0.2% (w/v) cetyltrimethylammonium tosylate (CTAT) and 0.8% sodium dodecylbenzenesulfonate (SDBS). Butyl methacrylate (BMA) and t-butyl methacrylate (t-BMA) were used as monomers and ethylene glycol dimethacrylate (EGDMA) as a cross-linking agent.

For loading the nanocapsules, a solution of water containing ~1-10 mM of a molecule to be encapsulated was used as the solvent (Figure 2A). Prior to polymerization, the vesicle size was monitored using dynamic light scattering (DLS) (Fig. 2B). A small size distribution centered at 100-200 nm was achieved either by ~2 h equilibration times or via extrusion. Following thermal polymerization (65°C for 8-12 h), nanocapsules were precipitated using methanol and then separated from the reaction solution by centrifugation and the decanting of the supernatant. The nanocapsules were washed extensively (>20 total washes) with methanol-water solutions, followed by water and acetonitrile.

SEM Analysis of freeze-dried[6,19] nanocapsules confirmed the presence of spherical nanocapsules within the desired size range (Fig. 2C). Nanocapsule pore sizes were estimated by encapsulation of three dyes (Fig. S1) that were used as size probes: Procion Red (1.1 nm), Nile Blue A (1.0 nm), and 4-(phenylazo)benzoic acid (0.6 nm) in a similar fashion to a previously published size probe retention assay.[5,20,] Following washing, Procion Red and Nile Blue A were shown to be retained by the nanocapsules, while 4-(phenylazo)benzoic acid was not suggesting an average nanocapsule pore size >0.6 nm and <1.0 nm. Using M06-2X/6-31G(d,p) geometry optimization and frequency calculations, the calculated diameters of the smallest cross-section of **1a** and **2a** were 1.01 and 1.40 nm, respectively, both of which were larger than the estimated nanocapsule pore size.

To demonstrate that **1a** and **2a** were unable to pass through the nanocapsules barrier, fluorescent derivatives were encapsulated and completely retained by the nanocapsules. Like DBTO, **1a** was not fluorescent, but the deoxygenation product of **1a**, i.e. the sulfide **1b,** was fluorescent. Nanocapsules loaded with **2a** could not be prepared since **2a** is not water-soluble; however, a water-soluble derivative of **2a**, i.e. **3**, was prepared and found to fluoresce. Fluorescence spectroscopy of **1b**-loaded nanocapsules and **3**-loaded nanocapsules was performed at an excitation wavelength (λ_{ex}) of 270 nm, with emission peaks at 368 and 344 nm, respectively. As shown in Fig. 3A-B, when compared to the spectra of **1b** and **3** alone, the results indicated that both **1b** and **3** were successfully encapsulated and retained after extensive washing. Since **3** had limited solubility in water, lower concentrations of **3** (≤1 mM) were used to prepare **3**-loaded nanocapsules, which was proposed as the cause of the weak emission observed for the **3**-loaded nanocapsules.

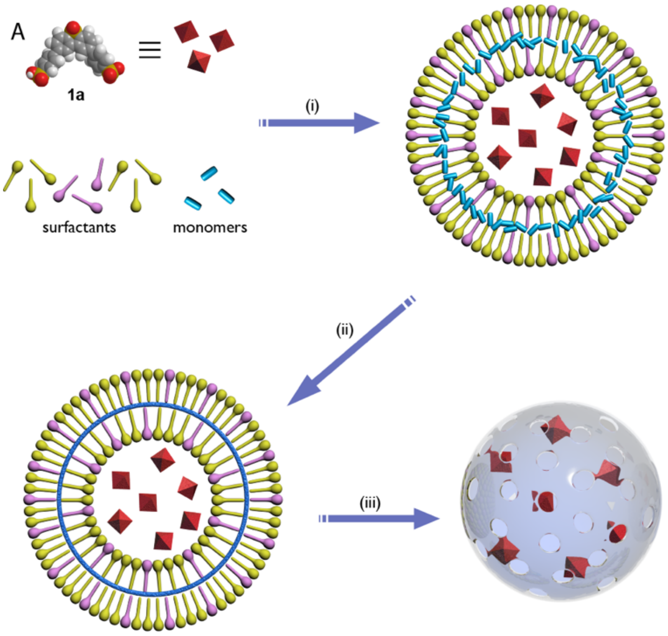

Nonetheless, the successful encapsulation of **1b** and **3** suggested that **1a** and **2a** are too large to pass through pores of the nanocapsule barrier, and thus, sufficient separation of **1a** and **2a** can be achieved.

Figure 2. Preparation of **1a**-loaded nanocapsules: (A) Self-assembly of surfactant vesicles with monomers migrating to the interior of the bilayers (i); polymerization (ii); washing step to remove surfactants and un-encapsulated **1a** (iii), (B) Typical size distribution (solid line) and autocorrelation function (open circles) of vesicles. The autocorrelation indicates the correlation of scattering intensity at one time with itself at a different time, which is closely related to the vesicle size, (C) Characterization of nanocapsules (freeze-dried) by SEM.

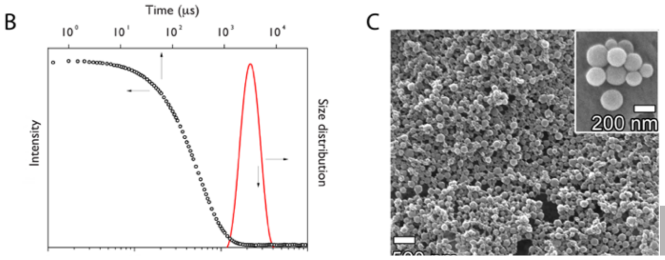

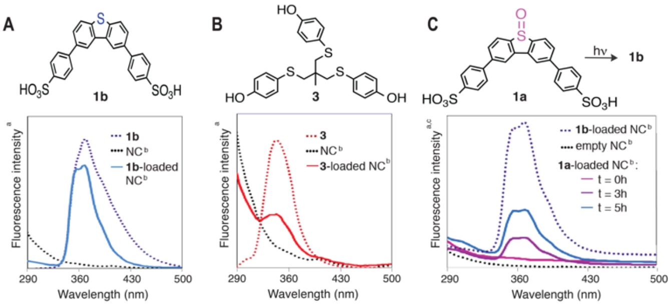

Figure 3. Evidence for separation and encapsulation: (A) Fluorescence spectra (λ_{ex}, 270 nm) showing encapsulation of DBT derivative, **1b**, in acetonitrile, (B) Fluorescence spectra (λ_{ex}, 270 nm) showing encapsulation of O(^{3}P)-trap derivative, **3**, in acetonitrile, (C) Fluorescence spectra (λ_{ex}, 270 nm) at various stages of irradiation of **1a**-loaded nanocapsules with comparisons to the "empty nanocapsules" and **1b**-loaded nanocapsules. a The fluorescence intensity scale was normalized to show all spectra. b Nanocapsules represented with the abbreviation, NC. c The relative fluorescence intensity for photolysis of 1a-loaded nanocapsules are depicted. All solutions were prepared in acetonitrile.

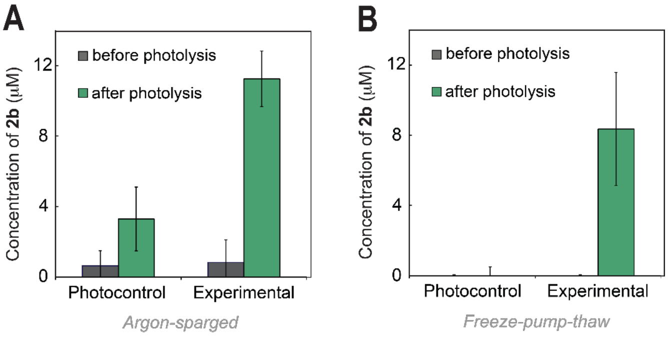

Figure 4. Evidence for a diffusing oxidant. The concentration of **2b** is given before and after photolysis of experimental solution, i.e. **1a**-loaded nanocapsules in the presence of **2a**, and photocontrol solution, i.e. **1b**-loaded nanocapsules of "empty" nanocapsules in the presence of **2a**; photolyzed 5h using broadly emitting fluorescent bulbs (fwhm, 325-375 nm). All error bars are given at a confidence level of 95%. Under argon-sparged conditions (A), each bar represents ≥6 trials. In freeze-pump-thaw trials (B), the concentration of **2b** was zero at t = 0 h, and each bar represents 3 trials.

1a-loaded nanocapsules were irradiated with broadly emitting UV light (fwhm, 325-375 nm), and fluorescence spectroscopy was performed at 0, 3, and 5 h (Fig. 3C). A fluorescence spectrum consistent with **1b**, increased over time, which demonstrated that encapsulation did not prevent photodeoxygenation of **1a**. After the last fluorescence spectra was taken, the nanocapsules were filtered off, and the HPLC analysis of the supernatant did not reveal any trace of **1a** or **1b**, indicating that no leakage occurred during photolysis. Together these results confirmed that **1a** is encapsulated and retained in the nanocapsules throughout photolysis.

To determine if the photodeoxygenation of **1a** generates a small diffusing oxidant, **1a**-loaded nanocapsules with **2a** present in the exterior solution were irradiated as shown in Figure 1. Nanocapsules loaded with **1a** were used for experimental trials, while **1b**-loaded nanocapsules and "empty" nanocapsules were used as two different types of photocontrol trials. Experimental and photocontrol trial solutions contained nanocapsules and 20 ± 2 mM of **2a** dissolved in acetonitrile. Two different degassing methods were examined: argon-sparging and freeze-pump-thaw. Degassing via argon-sparging is known to leave behind residual O$_2$, while a freeze-pump-thaw method can reduce O$_2$ to insignificant concentrations.[1] Degassed solutions were irradiated using broadly emitting fluorescent bulbs (fwhm 325-375 nm) for 5 h. By a procedure described in SI, the maximum concentration of **1a** (in nanocapsules) in the experimental solutions was estimated to be 8.5 mM or lower.

A total of twelve experimental and ten photocontrol trials were performed. Overall, the photolysis of **1a**-loaded nanocapsules in the presence of **2a** resulted in the formation of 8-11 μM of **2b**. Depending on the method of degassing, little (<3 μM) or no **2b** was observed in photocontrol experiments containing **2a** and **1b**-loaded nanocapsules or "empty" nanocapsules. The results of ≥6 trials for the photolysis of argon-sparged solutions (Fig. 4A) indicate that the average change in concentration of **2b** in experimental solutions was 10.4 μM, amounting to a 4x increase in **2b** formation in the experimental trials relative to the photocontrols. On average, the increase in **2b** observed in photocontrol experiments with "empty" nanocapsules was 2.7 μM. In photocontrol solutions containing **1b**-loaded nanocapsules, there was no increase in **2b** concentration. Three trials were performed under freeze-pump-thaw conditions for photocontrols and experimental trials (Fig. 4B). The initial concentration of **2b** was found to be zero in each trial. The photolysis of **1a**-loaded nanocapsules in the presence of **2a** resulted in the formation of 8.4 μM of **2b**, on average.

In the controls degassed by freeze-pump-thaw, where O$_2$ is presumably insignificant, there was no change in the concentration of **2b** after irradiation. Therefore, we attributed the formation of **2b** observed in the argon-sparged control experiments (Figure 2A, photocontrol) to the presence of residual O$_2$ in solution. In the absence of O$_2$, the oxidation of **2a** was only observed upon photolysis of **1a** in free solution or **1a**-loaded nanocapsules, confirming that the oxidant resulted from **1a** photodeoxygenation.

As a control, we examined if **2b** could be the result of a thermal reaction or direct photoproduct of **2a**. Minor photochemical degradation of **2a** was observed; however, **2b** was not observed in the absence of O$_2$. Using GC-MS, products of degradation were identified as thiophenol, diphenyl disulfide, 2,2-bis((phenylthio)methyl)-propane (**4a**), and 2,2-bis((phenylthio)methyl)-cyclopropane. In the dark under ambient air, **2a** was found to oxidize to **2b**; although, the process occurred very slowly over a period of a month.

In an additional control, a solution containing 80 μM **1a**, "empty" nanocapsules, and **2a** (degassed by freeze-pump-thaw) was photolyzed for 5 h, resulting in complete conversion of **1a** to **1b**. Following photolysis, the observed concentration of **2b** was 7.4 μM, or slightly less than the average observed in solutions containing **1a**-loaded nanocapsules. If **1a** leaked from **1a**-loaded nanocapsules to cause the oxidation of **2a** observed in experimental solutions, then the concentration of leaked **1a** would have to be at least 80 μM. The detection limit of **1a** and **1b** was found to be 0.5 μM, and neither **1a** or **1b** were observed in the supernatant following irradiation. Therefore, the increase in **2b** observed in the experimental trials cannot be explained by leakage of **1a**.

The polymer nanocapsules were measured to have a nanometer-thick shell,[6] which is about the size of the smallest cross-section of **1a** and **2a**. In the synthesis of rotaxane-like structures, a short linker threaded through a nanopore was not able to connect two molecules located on opposite sides of the shell.[21] This observation suggested that direct physical contact between **1a** and **2a** was extremely unlikely. Nevertheless, we considered a hypothetical scenario of physical contact between **1a** and **2a** through an event involving the partial insertion of **1a** and **2a** into the same small hole (or pore) on either side of the nanocapsule shell. Since **1a** has a rod-like shape and **2a** has a dendritic shape, the most likely collision event within the pore would be between the phenyl groups of **1a** and **2a**. This unlikely event of direct oxygen atom transfer would likely require arene oxide intermediates, but no phenolic products of **2a**, which would be expected for arene oxide intermediates, were observed in any experiment. A collision event between the sulfoxide of the excited **1a** and the sulfide of **2a** would be required for direct oxygen atom transfer resulting in **2b**. The probability of a productive collision event within a pore of the nanocapsules is very small and cannot explain the 8-11 μM increase in **2b**. The diffusion distance of O(^{3}P) in this system is predicted to be slightly less than 65 nm,[17] and thus, a freely diffusing O(^{3}P) would be capable of traversing the nanocapsule intact.

The results from the experiments described above demonstrate that photodeoxygenation of **1a** inside of the nanocapsules generates a freely diffusing intermediate that oxidizes **2a** to **2b.** The oxidation of **2a** to **2b** upon irradiation in the presence of O_2 (Figure 2A, photocontrol) raises the possibility that the intermediate formed could be O_2. While the current experiments cannot rule this out, the preponderance from previous studies have led to the conclusion that the direct irradiation of **DBTO** and its derivatives result in photodeoxygenation by a unimolecular mechanism.[1,2,(REFS)] A biomolecular mechanism of deoxygenation was inconsistent with several different experiments. Photodeoxygenation was observed for DBTO that had been isolated in a solid matrix to prevent bimolecular collisions.[1,2(more)] Additionally, the selective irradiation of **DBTO** in the presence of diphenyl sulfoxide produced no diphenyl sulfide, which would be expected if a bimolecular exciplex was involved in the photodeoxygenation mechanism.[1] The possibility of two O(^{3}P) combining to form O_2 is unlikely due to the low steady-state concentration of O(^{3}P) in these conditions.

As described in the supporting information (Table S1, Figure SX), a common intermediate and isolation experiment were performed. These experiments indicated that **1a** and **DBTO** generate an oxidant with the same chemoselectivity and **1a** undergoes photodeoxygenation by a unimolecular mechanism.

Applying Occam's razor, the simplest explanation of the oxidation of **2a** through an impermeable barrier upon irradiation of **1a** is that the photodeoxygenation of **1a** generates a small freely diffusing oxidant. Since **1a** undergoes deoxygenation by unimolecular mechanism and has same chemoselectivity as **DBTO**, these results are consistent with the identity of this freely diffusing oxidant as being O(^{3}P).

The employed experimental scheme answers a key mechanistic question about the nature of the oxidant in these photooxygenations. The experimental scheme also offers a viable method for studying other short-lived reactive intermediates.

We greatly acknowledge financial support by the National Science Foundation under CHE-1255270 and CHE-1709921. This work was additionally supported by the University of Connecticut Research Excellence Program.

Conflicts of interest

There are no conflicts to declare.

Notes and references

1 D. D. Gregory, Z. Wan, W. S. Jenks, *J. Am. Chem. Soc.* 1997, **119**, 94–102.

2 J. Korang, W. R. Grither, R. D. McCulla, *J. Am. Chem. Soc.* 2010, **132** 4466.

3 H. Kautsky, H. de Bruijn, *Naturwissenschaften* 1931, **19** 1043.

4 A. Greer, *Acc. Chem. Res.* 2006, **39**, 797.

5 M. D. Kim, S. A. Dergunov, E. Pinkhassik, *Langmuir* 2015, **31**, 2561.

6 A. G. Richter, S. A. Dergunov, M. D. Kim, S. N. Shmakov, S. V. Pingali, V. S. Urban, Y. Liu, E. Pinkhassik, *J. Phys. Chem. Lett.* 2017, **8**, 3630.

7 S. A. Dergunov, K. Kesterson, W. Li, Z. Wang, E. Pinkhassik, *Macromolecules* 2010, **43**, 7785.

8 A. Q. Maclin, M. D. Kim, S. A. Dergunov, E. Pinkhassik, *Electroanalysis* 2015, **27**, 733.

9 M. D. Kim, S. A. Dergunov, E. Lindner, E. Pinkhassik, *Anal. Chem.* 2012, **84**, 2695.

10 S. A. Dergunov, B. Miksa, B. Ganus, E. Lindner, E. Pinkhassik, *Chem. Commun. (Camb).* 2010, **46**, 1485.

11 L. T. Banner, D. C. Danila, K. Sharpe, M. Durkin, B. Clayton, B. Anderson, A. Richter, E. Pinkhassik, *Langmuir* 2008, **24**, 11464.

12 C. A. McKelvey, E. Kaler, J. A. Zasadzinski, B. Coldren, H. T. Jung, *Langmuir* 2000, **16**, 8285.

13 S. M. Omlid, A. Isor, K. L. Sulkowski, S. M. Chintala, J. T. Petroff, R. D. McCulla, *Synthesis (Stuttg).* 2018, **50**, 2359.

14 P. K. Dornan, P. L. Leung, V. M. Dong, *Tetrahedron* 2011, **67**, 4378.

15 K. B. Thomas, A. Greer, *J. Org. Chem.* 2003, **68**, 1886.

16 D. L. Singleton, R. J. Cvetanovic, *J. Phys. Chem. Ref. Data* 1988, **17**, 1377.

17 S. M. Omlid, M. Zhang, A. Isor, R. D. McCulla, *J. Org. Chem.* 2017, **82**, 13333.

18 M. D. Kim, S. A. Dergunov, A. G. Richter, J. Durbin, S. N. Shmakov, Y. Jia, S. Kenbeilova, Y. Orazbekuly, A. Kengpeiil, E. Lindner, S. V. Pingali, V. S. Urban, S. Weigand, E. Pinkhassik *Langmuir* 2014, **30**, 7061.

19 M. D. Kim, S. A. Dergunov, E. Pinkhassik, *Langmuir* 2017, **33**,

7732.

20 S. N. Shmakov, E. Pinkhassik, *Chem Commun.* 2013, **49**, 11026.

21 S. A. Dergunov, N. Ehterami, E. Pinkhassik, *Chem. Eur J.* 2016, **22**, 14137.